

Surface temperature retrieval in a temperate grassland with multiresolution sensors

S. J. Goetz, and R. N. Halthore

Hughes-STX Corporation, Greenbelt, Maryland

F. G. Hall and B. L. Markham

NASA Goddard Space Flight Center, Greenbelt, Maryland

Abstract. Radiometric surface temperatures retrieved at various spatial resolutions from aircraft and satellite measurements at the FIFE site in eastern Kansas were compared with near-surface temperature measurements to determine the accuracy of the retrieval techniques and consistency between the various sensors. Atmospheric characterizations based on local radiosonde profiles of temperature, pressure, and water vapor were used with the LOWTRAN-7 and MODTRAN atmospheric radiance models to correct measured thermal radiances of water and grassland targets for atmospheric attenuation. Comparison of retrieved surface temperatures from a helicopter-mounted modular multispectral radiometer (MMR) (~5-m “pixel”), C-130 mounted thematic mapper simulator (TMS) (NS001, ~20-m pixel), and the Landsat 5 thematic mapper (TM) (120-m pixel) was done. Differences between atmospherically corrected radiative temperatures and near-surface measurements ranged from less than 1°C to more than 8°C. Corrected temperatures from helicopter-MMR and NS001-TMS were in general agreement with near-surface infrared radiative thermometer (IRT) measurements collected from automated meteorological stations, with mean differences of 3.2°C and 1.7°C for grassland targets. Much better agreement (within 1°C) was found between the retrieved aircraft surface temperatures and near-surface measurements acquired with a hand-held mast equipped with a MMR and IRT. The NS001-TMS was also in good agreement with near-surface temperatures acquired over water targets. In contrast, the Landsat 5 TM systematically overestimated surface temperature in all cases. This result has been noted previously but not consistently. On the basis of the results reported here, surface measurements were used to provide a calibration of the TM thermal channel. Further evaluation of the in-flight radiometric calibration of the TM thermal channel is recommended.

1. Introduction

Retrieval of radiometric surface temperature from satellite and aircraft radiometers makes it possible to extend estimates of evapotranspiration and energy balance components over large regions [Price, 1982; Choudhury, 1989]. However, energy budget calculations are very sensitive to variations in surface temperature [Kustas *et al.*, 1989; Hall *et al.*, 1992]. For this reason it is important that remotely sensed thermal measurements be accurately corrected to retrieve surface temperature. Numerous factors need to be quantified in order to assess the accuracy of surface temperature retrieval, including sensor radiometric calibration [Wukelic *et al.*, 1989; Palmer, 1993], correction for atmospheric attenuation of the at-sensor signal [Price, 1983; Bartolucci *et al.*, 1988; Cooper and Asrar, 1989], correction for surface emissivity [Wukelic *et al.*, 1989; Norman *et al.*, 1990], characterization of spatial variability in ground cover [Hatfield *et al.*, 1984; Kustas *et al.*, 1990], and the combined effects of viewing geometry, background, and fractional vegetative cover [Kimes *et al.*, 1980; Norman *et al.*, 1990; Vining and Blad, 1992; Friedl and Davis, 1994].

Despite the extensive characterization of these factors, there are relatively few studies of temperature retrieval from multiple sensors at a single location, or of various targets over a range of viewing conditions (reviewed below). The objective of the current study was to retrieve and to compare surface temperatures from a variety of high spatial resolution satellite and aircraft-based remote sensing instruments across a range of spatial scales and to validate them with near-surface measurements. Early results were reported by Goetz *et al.* [1993]. A similar analysis was done by Markham *et al.* [1992] for surface reflectance retrieval. Field data used in this study were collected in 1987 and 1989 as part of First International Satellite Land Surface Climatology Project (ISLSCP) Field Experiment (FIFE). A detailed description of FIFE is given by Sellers *et al.* [1992].

2. Data Calibration and Correction Methodology

2.1. Data Sets

Measurements of surface temperature in the FIFE study area were collected from instruments on a variety of platforms. The temperatures compared in this study were collected from automated mesonet stations (AMSS) equipped with Everest

Copyright 1995 by the American Geophysical Union.

Paper number 94JD02684.
0148-0227/95/94JD-02684\$05.00

Table 1a. Image Data Acquired August 15, 1987

Platform-Sensor	UT	View Zenith	View Azimuth	Altitude	Nadir Resolution, m	Coincident Data
Landsat-TM	1633	4.1	281.0	706 km	120	NS001, Helo-MMR, mast IRT
C130-NS001	1622	±50	123/303	5183 m	13	TM, Helo-MMR, mast IRT
C130-NS001	1636	±50	123/303	5244 m	13	TM, Helo-MMR, mast IRT
C130-NS001	1645	±7	049/229	5366 m	13	TM, NS001 (reservoir)
Helicopter-MMR	1600-1701	0	0	300 m	5	NS001, mast IRT
Mast IRT	1622-1714	30	varied	2.5 m	0.6	NS001, Helo-MMR
AMS	1615-1715	0	0	1 m	0.3	all

model 4000 infrared thermometers (IRT), hand-held masts equipped with a Barnes modular multispectral radiometer (MMR) and Everest model 112 and model 4000 IRTs, a helicopter equipped with a Barnes MMR and Everest model 4000 IRT, a C-130 aircraft equipped with the NS001 thematic mapper simulator (TMS) and a Barnes precision radiation thermometer (PRT-5), and the Landsat 5 thematic mapper (TM). In addition, there were surface temperature measurements acquired with a PRT-5 from a boat on nearby Tuttle Creek Reservoir.

Radiometer data sets and the timing of acquisitions used in our analyses are summarized in Tables 1a and 1b. The spatial resolution (effective cell size) of the different sensors result in temperature differences if the proportion of background to vegetative signal varies within the field of view [Hatfield *et al.*, 1984; Kustas *et al.*, 1990]. The AMS IRTs and the mast-mounted IRT and MMR instruments have a 15°C field of view, resulting in a sampled surface area less than 1 m² from their respective heights, at a nadir view angle. The mast-mounted IRT data were collected at a 30° view zenith angle, parallel and perpendicular to the principal solar plane [Hays *et al.*, 1993], resulting in a sampled surface area of the order of 1 m². The mast-mounted MMR data used in our comparisons were all collected at nadir. Both the IRT and the MMR data were corrected for surface emissivity, measured at the site, and for downwelling longwave radiation [Hays *et al.*, 1993]. The AMS IRT data were converted from factory preset emissivity values of 0.98 to a value of unity emissivity using revised calibration coefficients [Blad *et al.*, 1990].

The helicopter-MMR data, acquired at an altitude of 230 m in 1987 and 300 m in 1989, are averaged over a few minutes as the helicopter hovered over the designated target [Walshall and Middleton, 1992]. The nominal ~5-m spot size (25 m²) of the helicopter MMR therefore is likely to include some contribution from surrounding targets, resulting in an effective area that is somewhat less than the NS001's 12- to 20-m pixels (144–400 m²). The TM 120-m pixel encompasses many times the area of the other instruments (14400 m²).

The best set of coincident thermal measurements at FIFE were on August 15, 1987, and August 4, 1989. On August 15, 1987, around 1630 UT, there are coincident acquisitions of Landsat 5 TM, NS001, helicopter MMR, and the mast-mounted IRT. On August 4, 1989, there are coincident acquisitions of Landsat 5 TM and NS001 around 1630 UT and NS001, helicopter MMR, and mast-mounted MMR around 1740 UT. Surface temperatures of Tuttle Reservoir are available on August 4, 1989, but not on August 15, 1987.

In addition to the intercomparison of the single-date data sets we also examined the relationship between measured and retrieved surface temperatures from the TM, NS001, and helicopter MMR on all other dates in both years when the remotely sensed data were coincident with surface measurements.

2.2. Radiometric Calibration

Current sensor radiometric calibrations of each of the instruments were applied to convert sensor digital counts to apparent at-sensor spectral radiances. Descriptions of the calibration procedures carried out as part of FIFE, including summaries by instrument, can be found in the work of *Halthore and Markham* [1992] and *Goetz et al.* [1992]. A more detailed discussion of the radiometric calibration of the thermal channel of the MMR and IRT instruments is reported by *Blad et al.* [1990].

Landsat 5 thematic mapper. The most recent vicarious calibration of the Landsat 5 TM thermal channel was conducted at the White Sands Missile Range in August 1992 [Palmer, 1993]. Retrieved TM surface temperatures and near-surface measured temperatures from an infrared radiative thermometer, both adjusted for surface emissivity, were used to reconstruct the TM prelaunch calibration to less than 5%, the equivalent of a 3.4°C temperature difference. Other reviews of the in-flight radiometric calibration of the Landsat 5 TM are discussed in section 4.

In this study, TM at-sensor spectral radiances (L , W m⁻² sr⁻¹ μm⁻¹) were calculated using the slope and intercept

Table 1b. Image Data Acquired August 4, 1989

Platform-Sensor	UT	View Zenith	View Azimuth	Altitude	Nadir Resolution, m	Coincident Data
Landsat-TM	1633	5.0	281.0	706 km	120	NS001
C130-NS001	1622	±50	178/358	8035 m	20	TM
C130-NS001	1726	±50	030/210	8107 m	20	Helo-MMR, mast-MMR
C130-NS001	1738	±7	146/236	8138 m	20	TM, NS001, boat-IRT (reservoir)
Helicopter-MMR	1720-1844	0	0	300 m	5	NS001, mast-MMR
Mast-MMR	1701-1747	0	varied	3.4 m	0.8	NS001, Helo-MMR
AMS	1615-1845	0	0	1 m	0.3	all

terms based on the TM internal calibration, obtained from the tape header, as

$$L = \text{count} * \text{slope} + \text{intercept} \quad (1)$$

where slope = $0.0563 \text{ W m}^{-2} \text{ sr}^{-1} \mu\text{m}^{-1}$ and intercept = 1.2378 counts. The Landsat data were received from EOSAT Corporation in the P-tape format.

NS001 thematic mapper simulator. Radiometric calibration of the thermal channel of the NS001 was not extensively evaluated as part of FIFE. However, on the basis of preliminary examination of water targets at a variety of altitudes with predawn data collected in August 1987 the NS001 appears to be stable through a range of external air temperatures (B. L. Markham, unpublished memorandum, May 1990). Because the NS001 views both the target and the internal blackbodies through the full optics, there were no changes in the instrument between 1987 and 1989 that should affect the thermal calibration.

NS001 at-sensor thermal radiances were derived from calibration coefficients obtained from a two-point calibration using the in-flight NS001 blackbody temperatures [Richard *et al.*, 1978]. Gains and offsets were calculated for each flight line and applied to calculate spectral radiances as

$$L = (\text{count} - \text{offset})/\text{gain}. \quad (2)$$

On August 15, 1987, gains averaged over each of the three flight lines used in our analysis varied between 52.31 to 52.68 counts/W $\text{m}^{-2} \text{ sr}^{-1} \mu\text{m}^{-1}$, and offsets varied from -429.32 to -432.53 counts. On August 4, 1989, averaged gains varied between 58.55 and 60.49 counts/W $\text{m}^{-2} \text{ sr}^{-1} \mu\text{m}^{-1}$ and offsets between -418.46 and -434.75 counts.

Modular multispectral radiometer. The MMR instruments used during FIFE were calibrated in 1987 [Markham *et al.*, 1988] and again in 1989, using the procedure of Jackson *et al.* [1983]. The surface MMR temperatures, as submitted to the FIFE Information System (FIS) were calculated with measured site-specific emissivities and downwelling longwave radiation [Hays *et al.*, 1993]. The helicopter-MMR temperatures were submitted to FIS as brightness temperatures, without corrections for surface spectral emissivity [Walthall, 1988].

Surface infrared radiative thermometer (IRT). Calibration of the Everest IRT's mounted on the mast and on the AMS platforms is reported by Blad *et al.* [1990]. The AMS IRT temperatures were calibrated from a factory preset emissivity value of 0.98 to an emissivity of 1.0 [Blad *et al.*, 1990] before being entered into FIS. In contrast to the AMS IRT data the mast IRT temperatures submitted to FIS were corrected for measured surface emissivity and downwelling longwave radiation [Hays *et al.*, 1993].

2.3. Correction for Atmospheric Attenuation

Correction of the at-sensor signal for atmospheric effects typically requires computation of both the atmospheric attenuation and the path radiance terms in the radiative transfer equation for a given atmospheric condition. However, it has been noted that under certain atmospheric conditions, atmospheric correction of remotely sensed thermal radiance data may not be required [Bartolucci *et al.*, 1988]. We explore here the conditions required for this hypothesis to be true.

If L is the at-sensor radiance, L_g the target (ground) radiance at the same wavelength, T the transmittance of the atmosphere, and L_a the path radiance, then

$$L = L_g T + L_a. \quad (3)$$

Atmospheric scattering and ground reflectance are neglected and the first term on the right-hand side accounts for the attenuation of the ground emission. Below in this section we discuss situations where the ground emissivity is less than 1 (that is, when the ground reflectance cannot be neglected); in such cases an additional term due to reflection of the atmospherically emitted downward irradiance (L_R) [see Wukelic *et al.*, 1989] was included.

For an isothermal atmosphere the path radiance term can be written as $L_a = (1 - T) B(\Theta)$, with $B(\Theta)$ representing the Planck function at temperature Θ of the atmosphere. Equation (3) then becomes

$$L = L_g T + (1 - T) B(\Theta). \quad (4a)$$

In real atmospheres, properties such as temperature, density, and composition vary considerably with height. In such cases the atmosphere can be divided into N isothermal layers, with N increasing as required for a better representation. Equation (3) can be written to reflect variation with height as

$$L = L_g \prod_{i=1}^N T_i + \sum_{i=1}^N (1 - T_i) B(\Theta_i) \frac{T}{\prod_{j=1}^i T_j}. \quad (4b)$$

Here the total atmospheric transmission (T) is equal to $e^{-\tau}$, where τ is the total optical thickness at the wavelength of the sensor band.

For an isothermal atmosphere of temperature Θ the at-sensor radiance would be the same as the ground-emitted radiance, so that $L = L_g = \epsilon_g B(\Theta_g)$, where ϵ_g is the ground emissivity. In such a case, (4a) then becomes

$$\epsilon_g B(\Theta_g) (1 - T) = (1 - T) B(\Theta) \quad (5)$$

and $\Theta = \Theta_g$ if $\epsilon_g = 1$. Thus atmospheric correction is not required when the temperature of the isothermal atmosphere is the same as that of the ground.

For a real atmosphere it can be shown from (4b) and using $L = L_g$ that atmospheric correction is not required if the ground temperature Θ_g is equal to an effective atmospheric temperature Θ_{eff} , where the latter is defined as

$$B(\Theta_{\text{eff}}) = \frac{1}{(e^\tau - 1)} \left[\sum_{i=1}^N (1 - e^{-\tau_i}) B(\Theta_i) \exp \left(\sum_{j=1}^i \tau_j \right) \right]. \quad (6)$$

Here τ_i is the value of optical thickness for the i th layer and $\epsilon_g = 1$. Only under special circumstances (that is, when $B(\Theta_{\text{eff}}) = \epsilon_g B(\Theta_g)$) would we expect atmospheric correction to be unnecessary for surface temperature retrieval from remotely sensed observations.

2.4. Atmospheric Characterization

During FIFE, atmospheric properties of temperature, pressure, humidity, and wind velocity as a function of height were measured with on-site radiosonde profiles [Brutsaert, 1991]. The radiosonde profiles sample at many more levels in the atmosphere (about 300) than is necessary for radiative transfer calculations. Resampling of the radiosonde data set at height intervals that are smaller nearer the ground (where the density

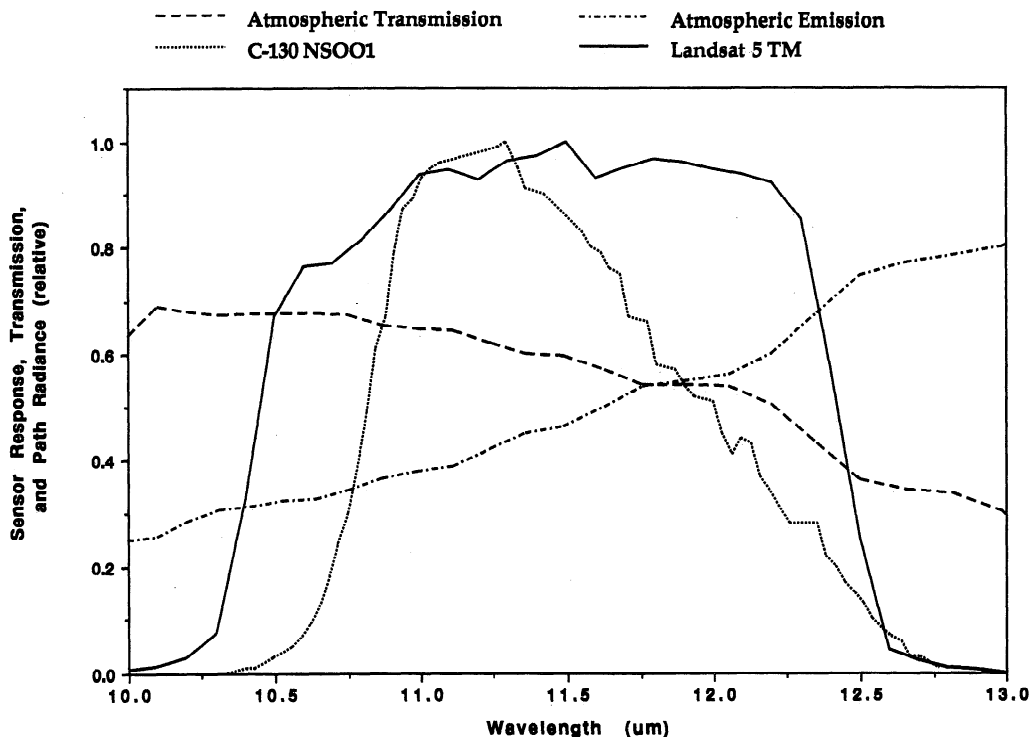


Figure 1. Variation of sensor response, atmospheric transmission, and path emission with wavelength. Units of sensor response and path emission are relative.

is higher) was done to reduce the number of levels to about 20. Since the sondes were not tracked above about 5 km, it is necessary to augment the atmospheric profiles of temperature and humidity with standard atmospheric profiles extending to about 100 km. Typically, 14 such levels were obtained from a standard atmospheric model to bring the total number of levels to 34, the maximum allowed in the radiative transfer codes.

The atmospheric radiative transfer models LOWTRAN-7 [Kneizys *et al.*, 1988] and MODTRAN [Berk *et al.*, 1989] were used in the thermal radiance mode with the radiosonde-augmented profiles and relevant viewing geometry to perform the radiative transfer in the atmosphere. The major difference between the two radiative transfer models is the spectral resolution, which is specified as 20 and 2 cm^{-1} , respectively. The models compute the transmission and the path radiance as a function of wavelength. Band transmittance (T) and spectrally averaged path radiance (L_a) were then computed for the whole band by integrating the model outputs weighted by the sensor response function for each of the TM, MMR, and NS001 sensor bands (Figure 1).

On August 15, 1987, and August 4, 1989, radiosonde measurements were available coincident with the TM and the airborne MMR and NS001 acquisitions. In the case of the NS001, L_a and T vary with scan angle as a result of variable pathlength through the atmosphere. For example, band-integrated values of L_a and T across the 100° NS001 scan at 1622 UT on August 4, 1989, vary from $L_a = 3.53 \text{ W m}^{-2} \text{ sr}^{-1}$, $T = 0.59$ at nadir to $L_a = 4.68 \text{ W m}^{-2} \text{ sr}^{-1}$, $T = 0.46$ at 50° off nadir. Derived atmospheric optical properties for each instrument are discussed further in section 3.

Although estimates of total atmospheric column precipitable water were not directly used in any of the atmospheric corrections, the values derived from the radiosonde specified

atmospheres in the MODTRAN model are worth noting for comparison purposes. On August 15, 1987, precipitable water between the surface and the top of the atmosphere was 3.44 cm. On this date the maximum height of the radiosonde profile was 5.8 km. On August 4, 1989, both the precipitable water and the maximum height of the sounding were slightly less, at 3.28 cm and 4.3 km, respectively.

2.5. Surface Temperature Retrieval

In the discussion that follows uncorrected or apparent temperature (Θ_u) refers to the temperature derived from the at-sensor radiance (L) without atmospheric correction. Corrected brightness temperature (Θ_c) refers to temperatures derived from atmospherically corrected radiance (L_c), and retrieved surface temperature (Θ_g) refers to temperatures derived from ground-emitted radiance (L_g) corrected for reflection of downwelling longwave radiation and $\varepsilon_g \neq 1$. Note that $L_g = L_c$ when $\varepsilon_g = 1$.

For comparison, the spectral radiances were corrected for $\varepsilon_g \neq 1$ only in those cases where the surface measurements were also corrected (e.g., the mast-mounted IRT and MMR). In comparisons with the AMS platforms the retrieved satellite and aircraft surface temperatures were not corrected for variations in ε_g since the AMS-IRT temperatures were calculated assuming $\varepsilon_g = 1$.

At the FIFE site, Palluconi *et al.* [1990] found that ε_g varies little with either emission angle (between 0° and 60°C), land use (grazed-ungrazed, burned-unburned), or phenology. They measured $\varepsilon_g = 0.99 \pm 0.01$, with very small (0.005) variation with wavelength between 8 and 12 μm . Blad *et al.* [1990] also measured ε_g at FIFE, over a range of sites, and found variations between 0.96 and 0.99. In those cases where the remotely sensed data were being compared with near-surface measure-

ments corrected for ε_g , the same value of ε_g was used in both the near-surface and the remotely sensed temperature calculations.

For direct sensor-to-sensor and sensor-to-surface comparisons, measured radiances were used to calculate corrected brightness temperature (Θ_c , °K) as

$$\Theta_c = \frac{K_2}{\ln(K_1/L_c) + 1} \quad (7)$$

where K_1 and K_2 (Table 2) are parameters derived from the spectral calibration of the instruments and Planck's equation [after Markham and Barker, 1986]. A comparison with the Planck function shows that $K_1 = hc/k\lambda$ and $K_2 = 2hc^2/\lambda^5$, where h is the Planck constant, c is the speed of light, k is the Boltzman constant, and λ is the appropriate effective wavelength of the observation band. Since the effective wavelength of the band depends on the temperature of the surface emission (a small effect) and wavelength dependence of the atmospheric transmission and emission (a larger effect), it is necessary to compute K_1 and K_2 empirically. This was done as follows:

Substituting for L_g from (3) into L_c in (7) for $\varepsilon_g = 1$, we obtain

$$\Theta_g = K_2 / \ln \left(1 + \frac{K_1 T \varepsilon_g}{L - L_a - L_R} \right) \quad (8)$$

where L_R is the reflected portion of downward irradiance.

Transmission T and path radiance L_a in the sensor band are calculated with MODTRAN for an initial $\Theta_g = 0$ ground temperature. By running MODTRAN again for two different values of Θ_g and obtaining the corresponding values of the at-sensor radiance (L), K_1 and K_2 are derived. The two ground temperatures are chosen to encompass typical values of the ground temperature observed at the Konza Prairie. A check of K_1 and K_2 is obtained by running MODTRAN with an assumed value of Θ_g to obtain L , then substituting L in (8) to obtain predicted Θ_g . The values of K_1 and K_2 , so derived, and given in Table 2, were found to be insensitive to different types of atmosphere used: midlatitude summer profile, tropical profile, or midlatitude winter profile. Also, the derived temperatures using (7) were found to agree to within $\pm 0.2^\circ$ for K_1 and K_2 determined from LOWTRAN-7 and from MODTRAN.

3. Comparison of Retrieved Surface Temperatures

Surface temperatures were retrieved for water targets at the Tuttle Reservoir and at grassland sites across the FIFE study area. Remotely sensed reservoir temperatures were compared to boat-mounted IRT measurements averaged across sample transects ranging from 250 m to 1 km in length on August 4, 1989. A Barnes PRT-5 mounted on the C-130 was used to examine the magnitude of the atmospheric corrections over

Table 2. Coefficients to Convert Spectral Radiance to Radiative Temperature

Platform-Sensor	K_1 , $\text{W m}^{-2} \text{sr}^{-1} \mu\text{m}^{-1}$	K_2 , °K
Landsat 5 TM	637.64	1270.53
C-130 NS001	625.00	1265.60
Helicopter MMR	678.50	1287.60

Table 3a. Uncorrected and Retrieved Surface Spectral Radiances and Radiative Temperatures of Tuttle Creek Reservoir, August 15, 1987

Variable	Landsat 5 TM	C130 NS001 (minimum)	C130 NS001 (maximum)
UT	1633	1645	1645
View zenith	3.5	± 7	± 7
View azimuth	281	049	229
L	9.235	8.928	9.042
Θ_u	25.86	23.75	24.62
L_a	3.578	3.666	3.666
T	0.576	0.584	0.584
L_c	9.821	9.005	9.200
Θ_c	30.19	24.34	25.82

Angles arc in decimal degrees, radiances in $\text{W m}^{-2} \text{sr}^{-1} \mu\text{m}^{-1}$, and temperatures in degrees Celsius. Symbols are as defined in the text.

the reservoir by comparing atmospherically corrected and uncorrected C-130 NS001 data to the coincident C-130 PRT-5 measurements.

Corrected brightness temperatures of grassland targets were compared to down-looking radiometers mounted on AMS stations throughout the study area coincident with the Landsat 5 overpass. Retrieved surface temperatures were compared to near-surface measurements at one site on each date the surface measurements were available. It should also be noted that the radiosondes were launched within the study area, close to the grassland sites, but approximately 10 km from the reservoir.

3.1. Water Targets

All comparisons over the water targets are between corrected brightness temperatures. In the analysis that follows, it should be kept in mind that the field of view of the Barnes PRT-5 is 15° , which results in a "swath width" from an altitude of 5 km over the reservoir of 1.3 km. In comparison, the NS001 scans over a 100°C field of view, resulting in a swath width of 12.5 km from the same altitude, from which the center 2 km was sampled for comparison to the boat transect.

August 15, 1987. Since no surface measurements were available over Tuttle Reservoir on August 15, 1987, we can only compare corrected brightness temperatures from the aircraft and satellite acquisitions. Corrected brightness temperatures of the reservoir from the TM and NS001 are presented in Table 3a. Two values are provided for the NS001, representing the range of observations during the time of the data acquisition. The C-130 PRT-5, acquiring data simultaneously with the NS001, recorded an apparent temperature of $26.8^\circ \pm 1.5^\circ\text{C}$ from an altitude of 5 km, which is 2.2° – 3.1°C warmer than the range of NS001 apparent temperatures. The difference between the C-130 PRT-5 and NS001 values is most likely caused by a combination of radiometric differences between the instruments and, to a lesser extent, differences in spatial sampling. The temperature difference between atmospherically corrected versus uncorrected NS001 data is 0.6° – 1.2°C , resulting in a corrected brightness temperature of the reservoir between 24.3° and 25.8°C .

The TM digital count value was identical for all samples of the reservoir (142), a result of the large field of view of the instrument (120 m) and coarse quantization of the data. The TM apparent temperature is 1.2° – 2.1°C warmer than the NS001 apparent temperatures and 1°C cooler than the C-130

Table 3b. Same as Table 3a but for August 4, 1989

Variable	Landsat 5 TM	C130 NS001 (minimum)	C130 NS001 (maximum)
UT	1633	1738	1738
View zenith	3.5	±7	±7
View azimuth	281	236	146
L	9.235	9.026	9.163
Θ_u	25.86	24.50	25.54
L_a	3.525	3.545	3.545
T	0.591	0.594	0.594
L_c	9.662	9.235	9.465
Θ_c	29.02	26.09	27.81
Θ_c -PRT5	+2.52*	-0.41	+1.31

*Acquired ~1 hour before the surface PRT5 measurements.

PRT-5. The TM corrected brightness temperature is 4.4°–5.8°C warmer than the NS001 corrected brightness temperatures. The temperature difference between atmospherically corrected versus uncorrected TM data is of the expected magnitude (+4.3°C), but the correction results in retrieved temperatures that deviate further from the corrected NS001 temperatures.

August 4, 1989. Water surface temperatures measured from a boat with a PRT-5 allow comparisons of the aircraft and satellite corrected brightness temperatures with surface measurements on this date. Measured surface temperature from the boat PRT-5 between 1720 and 1740 UT was $26.5 \pm 0.29^\circ\text{C}$. Corrected brightness temperatures of the Tuttle Creek Reservoir from the TM and NS001 are presented in Table 3b. The C-130 PRT-5 recorded an apparent at-sensor temperature of $24.1^\circ \pm 0.08^\circ\text{C}$ from an altitude of 8 km, which is 2.4°C cooler than the coincident boat-measured temperature. The discrepancy between the surface and the aircraft PRT-5 measurements is caused predominantly by atmospheric attenuation of the airborne PRT-5 signal. The C-130 PRT-5 is 0.4°–1.4°C warmer than the range of NS001 apparent temperatures, which is closer than that observed on August 15, 1987.

The NS001 acquisition is coincident with the boat measurements, and the apparent temperatures are 1.0°–2.0°C cooler than the surface measurements. After atmospheric correction the range in the NS001 brightness temperatures bracket the measured surface temperature (from -0.4° to +1.3°C). The temperature difference between atmospherically corrected versus uncorrected NS001 data is 1.6°–2.3°C, with the correction resulting in brightness temperatures closer to the surface-measured brightness temperature. The magnitude of the correction is consistent with the higher altitude the C-130 was flown in 1989 (Tables 1a and 1b).

The TM apparent temperature is 0.6°C cooler than the corresponding surface measurements. The TM corrected brightness temperature, obtained an hour before the boat measurements, is 2.5°C higher than the surface measurements. Correction of the TM data results in corrected brightness temperatures that deviate further from both the surface-measured temperature and the NS001 corrected brightness temperature, with atmospheric correction increasing the uncorrected temperature slightly less than observed August 15, 1987 (+3.2°C). It should be noted that the atmospheric properties derived over the respective bandwidths of the NS001 and the TM are similar, both in 1987 and 1989.

3.2. Grassland Targets

Helicopter MMR, C-130 NS001, and Landsat 5 TM were compared at all grassland sites with coincident surface temperature measurements on several days throughout 1987 and 1989. A centrally located site with additional near-surface measurements provided the best single intercomparison data set in both years (from a mast-mounted IRT at site 16 in 1987 and a mast-mounted MMR at site 916 in 1989). In the results that follow, the intercomparison at the centrally located site is presented in detail, followed by a more general intercomparison of the remainder of the available sites on August 15, 1987, and August 4, 1989, and then at all other available sites on several additional dates in both years.

Both corrected brightness temperature and retrieved surface temperature comparisons are presented because together they provide an indication of the magnitude of the emissivity correction. They also reflect the form in which the data were available to us.

August 15, 1987. Table 4a summarizes corrected brightness temperatures and retrieved surface temperatures at site 16. Two NS001 flights were acquired within minutes of the Landsat overpass time. In addition, temperatures were measured with the helicopter MMR and with a mast-mounted IRT during the same time period, making it the single best multi-sensor thermal data set available from FIFE. Unfortunately, no NS001 data were acquired over the prairie later in the day, which results in a lack of data at the warmest part of the day and therefore in a lower dynamic range of temperatures over the site. This limits the range of temperatures over which we can test the correction methodology on this date.

Surface temperature measurements acquired with the mast-mounted IRT between 1624 and 1714 UT ranged from 31.6° to 35.8°C over 11 subplots, with an average of $33.5^\circ \pm 1.02^\circ\text{C}$. AMS temperatures over the same time period ranged from 29.1° to 31.0°C, averaging 30.0°C. The mast-mounted IRT data are 3.5°C higher than the radiative temperatures measured at the corresponding AMS platforms, which reflects the correction of the mast-mounted IRT temperatures for a surface emissivity value of 0.98. Although the mast-mounted IRT data were collected around the AMS platforms, they are also representative of a larger area than the AMS IRT.

Apparent temperature from the helicopter MMR was 32.8°C, and the corrected helicopter MMR brightness temper-

Table 4a. Uncorrected and Retrieved Surface Spectral Radiances and Radiative Temperatures of a Continuous Vegetation Target (Site 16), August 15, 1987

Variable	Landsat 5 TM	C130 NS001	C130 NS001	Helicopter MMR
UT	1633	1622	1635	1634
View zenith	3.9	31.3	4.6	0
View azimuth	281	303	123	0
L	9.911	9.439	9.678	10.234
Θ_u	30.84	27.61	29.39	32.76
L_a	3.578	4.061	3.657	1.250
T	0.576	0.538	0.585	0.867
L_c	10.995	9.987	10.284	10.362
Θ_c	38.45	31.64	33.78	33.65
Θ_c -AMS	+8.45	+1.64	+3.78	+3.65
Θ_g	39.77	32.90	35.05	34.91
Θ_g -mast IRT	+6.23	-0.64	+1.51	+1.37

Units are the same as Table 3. Symbols are as defined in the text.

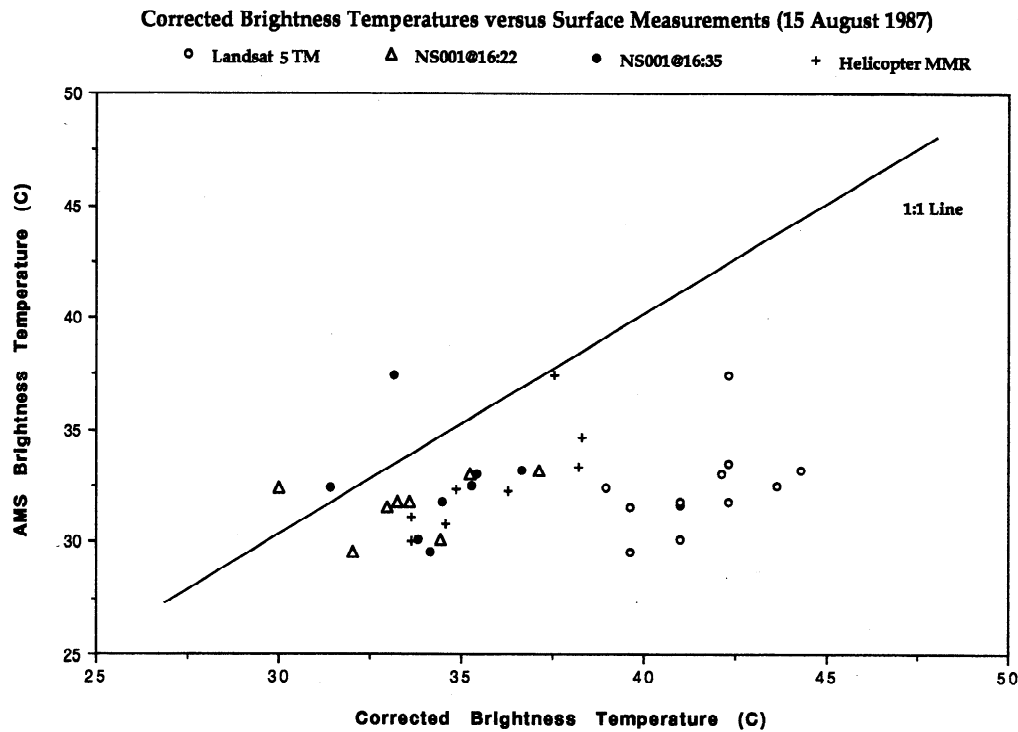


Figure 2. Corrected brightness temperatures and coincident surface AMS-IRT measurements on August 15, 1987.

ature was 33.6°C, a correction of less than 1°C. Correction for surface emissivity and downwelling longwave (3) results in a retrieved surface temperature of 34.9°C. The corrected brightness temperature is 3.6°C warmer than the corresponding AMS temperature, and the retrieved surface temperature is 1.4°C warmer than the corresponding mast-mounted IRT.

Atmospherically corrected NS001 brightness temperatures ranged from 31.6° to 33.8°C, a correction of approximately 4°C. Retrieved NS001 surface temperatures ranged from 32.9° to 35.0°C. The corrected NS001 brightness temperatures are 1.6°–3.8°C warmer than the corresponding AMS temperature, but the range of retrieved NS001 surface temperatures encompass the corresponding surface IRT temperature.

The TM apparent temperature is within 1°C of the AMS temperature. However, correcting the TM data increases the brightness temperature 7.6°C, which is 8.4°C warmer than the corresponding AMS value. The retrieved TM surface temperature is 6.2°C warmer than the corresponding mast-mounted IRT.

Comparison of TM, NS001, and MMR corrected brightness temperatures at other sites within the study area where coincident AMS measurements were available (Figure 2) is consistent with the results at site 16. The average deviation of the corrected helicopter MMR brightness temperatures from the corresponding AMS temperatures is +3.1°C. The NS001 brightness temperatures deviate +1.3°C on average, and the TM brightness temperatures deviate +7.9°C.

August 4, 1989. Table 4b summarizes retrieved surface temperatures at site 916 for two time periods, one coincident with near-simultaneous Landsat and NS001 acquisitions and one coincident with near-simultaneous mast-mounted and helicopter-mounted MMR acquisitions one hour later. One NS001 flight was acquired 11 min before the Landsat overpass

time, and the other was acquired 15 min before the helicopter MMR.

In 1989 the AMS and surface MMR measurements were made at different portions of the site. AMS temperatures from 1615 to 1645 UT ranged from 29.6° to 30.5°C, with an average of 30.1°C. An hour later, between 1715 and 1745 UT, the average AMS temperature at the site was 31.6°C. Surface temperature measurements acquired with a mast-mounted MMR between 1701 and 1747 UT ranged from 32.2° to 37.3°C over five subplots, with an average of 34.9°C. The surface MMR temperature is 3.3°C warmer than the AMS temperature, which again reflects the correction for surface emissivity

Table 4b. Same as Table 4a but for Site 916, August 4, 1989

Variable	Landsat 5 TM	C130 NS001	Helicopter MMR	C130 NS001
UT	1633	1622	1741	1726
View zenith	5.0	18.0	0	10.3
View azimuth	281	358	0	210
L	9.821	9.385	10.542	9.716
θ_u	30.18	27.21	34.89	29.67
L_a	3.525	3.640	1.377	3.557
T	0.591	0.583	0.859	0.592
L_c	10.653	9.859	10.669	10.398
θ_c	36.09	30.71	35.77	34.59
θ_c -AMS	+5.99	+0.61	+4.17	+2.99
θ_g	38.73	33.24	39.23	37.20
θ_g -MMR	+4.18*	-1.31*	+3.71†	+1.68

*Acquired approximately 45 min before the surface modular multi-spectral (MMR) measurements.

†Acquired at the end of the surface MMR data collection.

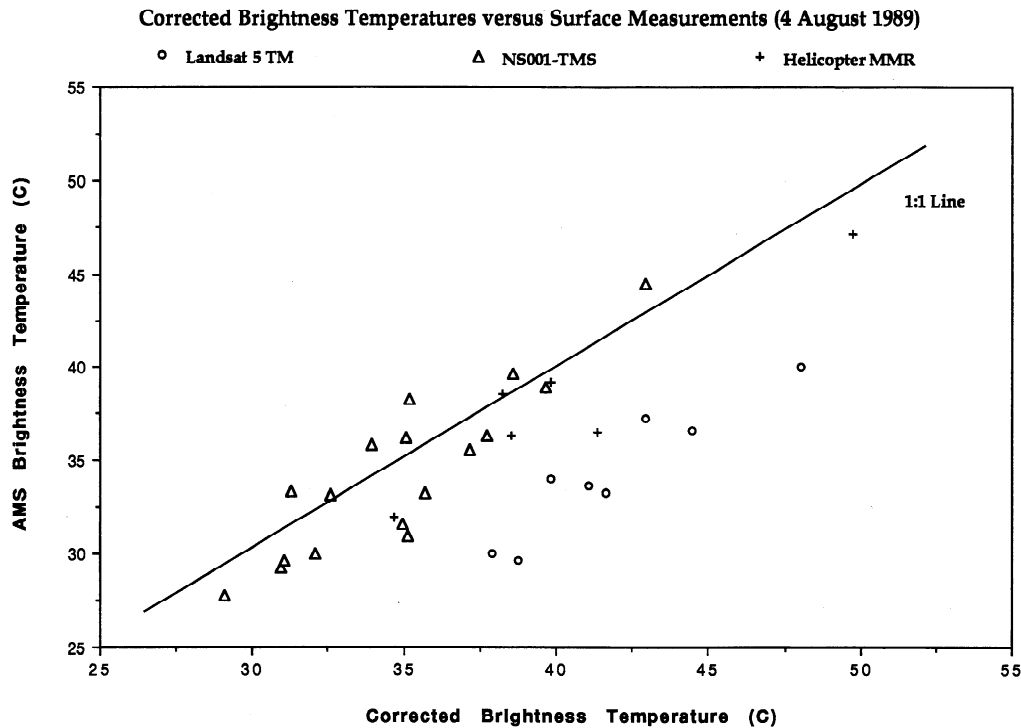


Figure 3. Corrected brightness temperatures and coincident surface AMS-IRT measurements on August 4, 1989.

(0.964), as well as the fact that the AMS IRT was located in a more densely vegetated portion of the site in 1989.

Apparent temperature from the NS001 at the time of the Landsat overpass was 27.2°C, approximately 3°C cooler than the TM temperature. Correcting for atmospheric attenuation increased the NS001 brightness temperature 3.5°C to within 0.6°C of the AMS. The retrieved NS001 surface temperature is 1.3°C cooler than the corresponding surface MMR temperature, which is consistent with the MMR data being collected some 40 to 60 min later in the morning (surface MMR = $34.55^\circ \pm 0.64^\circ\text{C}$ for 10 observations between 1701 and 1715 UT).

Correcting the TM data again results in an overestimation of the AMS surface temperature by 6°C, the same magnitude as the atmospheric correction. Similarly, the retrieved TM surface temperature is 4.2°C warmer than the corresponding surface MMR, even though the TM was acquired earlier in the morning.

Apparent temperature from the later NS001 flight is over 5°C cooler than the coincident helicopter MMR temperature. Correction of the NS001 and helicopter MMR data results in retrieval of brightness temperatures that are 3°C and 4°C warmer, respectively, than the corresponding AMS value. The retrieved NS001 and helicopter MMR surface temperatures are 1.7°C and 3.7°C warmer, respectively, than the mast-MMR value (surface MMR = $35.52^\circ \pm 0.76^\circ\text{C}$ for 15 observations between 1730 and 1749 UT). Note that the NS001 data were acquired at the beginning of the surface MMR data collection period, whereas the helicopter MMR data were acquired at the end of the surface data collection period.

When extended to other sites where coincident AMS measurements were acquired (Figure 3), the comparisons among TM, NS001, and MMR are consistent with those observed at site 916. The corrected helicopter MMR brightness tempera-

tures deviate on average +1.9°C from the AMS temperatures. The NS001 corrected brightness temperatures on this date are in better agreement with the AMS data than on August 15, 1987, deviating on average only +0.7°C. The corrected TM brightness temperatures also deviate less than was observed on August 15, 1987, but are still systematically 5.6°C warmer than the corresponding AMS temperatures.

The coincident NS001 and helicopter-MMR corrected brightness temperatures are in good agreement across a range of temperatures ($R^2 = 0.86$), but the MMR is systematically higher than the NS001 by 1.3°C. Additional radiative temperature measurements from an IRT mounted on the helicopter in 1989 agree with the uncorrected helicopter-MMR to within less than 0.6°C RMSE, which suggests the MMR values are properly calibrated.

3.3. Multidate Analysis

To extend the single-date analyses of August 15, 1987, and August 4, 1989, over the full range of observed temperature data collected during FIFE, all TM and helicopter MMR data, and a subset of the NS001 data acquired coincident with AMS and mast-mounted MMR and IRT measurements were examined. The results of brightness temperature comparisons with the AMS platforms are summarized in Table 5a, and the results of retrieved surface temperature comparisons with the corresponding mast-mounted MMR and IRT values are summarized in Table 5b.

Because the mast-mounted MMR and IRT measurements of surface temperature were found to be essentially identical on those days when both were collected together, they are used interchangeably. Nearly all the helicopter-MMR data were acquired coincident with mast-mounted MMR data, and all but one of the NS001 acquisitions were acquired coincident with mast-mounted IRT data. Thus issues related to the com-

parability of the mast-IRT and mast-MMR will not significantly alter the results of the multirate comparisons.

Helicopter modular multispectral radiometer. One hundred coincident helicopter MMR and AMS acquisitions (70 sites on 12 dates in 1987 and 30 sites on 6 dates in 1989) were analyzed. The radiosonde-specified atmospheric correction of the two dates previously reported (16 acquisitions) were included with the data from the additional dates, which were corrected using the midlatitude summer model of LOWTRAN-7.

Because the helicopter data were acquired only 230 to 300 m above ground level, the average magnitude of the atmospheric correction of the helicopter MMR data is small (+0.4°C). The apparent MMR temperatures averaged 2.8°C warmer than the AMS temperatures, and the corrected brightness temperatures averaged 3.2°C warmer than the AMS (Figure 4) ($R^2 = 0.91$).

A total of 11 coincident helicopter MMR and mast-mounted MMR acquisitions (6 sites on 4 dates in 1987 and 5 sites on 5 dates in 1989) were analyzed. The retrieved helicopter surface temperatures are in close agreement (+0.9°C) with the corresponding surface MMR measurements (Figure 4) ($R^2 = 0.97$).

NS001 thematic mapper simulator. The NS001 acquisitions were all corrected with radiosonde specified atmospheric, using the procedure described in section 2.3. The magnitude of the atmospheric correction parameters (L_p , τ) varies significantly with both pathlength (view angle) and time of year (Figures 5a and 5b). The largest values of L_p and the smallest values of τ for the dates observed here occurred in late summer (August). The inverse situation was noted in mid-October, and the midlatitude summer model was midway between the two.

As expected, the magnitude of the NS001 atmospheric corrections varied widely, from a minimum of 1.7°C to a maximum of 8.4°C (average = 4.0°C). Apparent, corrected, and retrieved surface temperatures are shown in Figure 6. The NS001 apparent temperature was 2.3°C cooler than the corresponding AMS temperatures, with an increasing tendency to underestimate at higher temperatures. The corrected NS001 brightness temperatures covary strongly with the surface AMS temperatures ($R^2 = 0.92$) but like the helicopter MMR are biased toward overestimation (+1.7°C). Correction of the most deviant at-sensor temperature (10°C cooler than the AMS) resulted in a brightness temperature estimate within 1.5°C of the AMS value.

Table 5a. Multirate Temperature Comparisons to Automated Mesonet Station Infrared Thermometer (IRT) Measurements

	Landsat 5 TM	NS001-TMS	Helicopter-MMR
AMS	28.38	28.78	28.40
Sample size	67	65	100
Θ_u	27.60	26.48	31.21
Θ_u -AMS	-0.78	-2.30	2.81
R^2	0.79	0.92	0.91
RMSE	2.60	1.60	1.87
Θ_c	33.70	30.45	31.64
Θ_c -AMS	5.32	1.67	3.24
R^2	0.79	0.92	0.91
RMSE	2.61	1.94	2.04
Θ_c - Θ_u	6.10	3.97	0.43

All temperatures are averages in degrees Celsius. Symbols are as defined in the text.

Table 5b. Multirate Temperature Comparisons to Mast-Mounted MMR and IRT Measurements, Otherwise Same as Table 5a

	Landsat 5 TM	NS001-TMS	Helicopter-MMR
Mast MMR, IRT	32.47	30.22	29.63
Sample size	3	8	11
Θ_u	29.10	25.29	29.63
Θ_u -mast	-3.37	-4.93	-1.51
R^2	...	0.96	0.97
Θ_g	37.03	30.22	32.07
Θ_g -mast	4.56	0.28	0.93
R^2	...	0.98	0.97
RMSE	...	1.24	1.24
Θ_g - Θ_u	7.93	4.93	2.44

A total of 7 coincident NS001 and mast-mounted IRT acquisitions, all in 1987, were analyzed. One additional site with coincident NS001 and mast-mounted MMR data, from August 4, 1989, was included in the analysis. The retrieved NS001 surface temperatures are in close agreement (+0.3°C) with the corresponding mast-mounted MMR and IRT measurements (Figure 6, $R^2 = 0.98$).

Landsat 5 thematic mapper. One of the eight TM scenes acquired of the FIFE site (April 9, 1987) had no coincident AMS measurements available. Five of the remaining seven had no radiosonde data available for atmospheric correction and were corrected with the midlatitude summer model of LOWTRAN-7. The remaining two TM scenes (August 15, 1987, and August 4, 1989) were corrected with radiosonde data, as previously described. Other TM scenes were acquired over the FIFE site in 1988, but no radiosonde data were available for correction, and the AMS data were as yet unavailable through the FIFE Information System.

The magnitude of the atmospheric correction of the TM data ranged from 1.9° to 9.6°C, averaging 6.1°C. These values are consistent with another study for which both uncorrected and corrected TM brightness temperatures were provided [Wukelic et al., 1989]. Apparent, corrected, and retrieved surface temperatures are shown in Figure 7. The TM apparent temperatures averaged 0.8°C cooler than the AMS measured temperatures, whereas the corrected brightness temperatures averaged 5.3°C warmer than the AMS values ($R^2 = 0.79$).

Only one additional site with coincident mast-mounted MMR or IRT data was available for comparison to retrieved TM surface temperatures. On July 14, 1987, mast-mounted MMR data were collected at site 42 at the time of the Landsat overpass. Since there were no radiosonde data available for atmospheric correction on this date, we have less confidence in the absolute retrieval of surface temperature. However, the retrieved TM surface temperature overestimation of near-surface observed temperature (+3.3°C) is consistent with the findings of the other dates.

4. Discrepancies With the Landsat 5 TM

Thermal comparisons of the Landsat 5 TM over grassland sites suggest that the TM temperatures systematically overestimate coincident surface AMS measurements by +5.3°C (Figure 7). Surface temperature retrievals over water targets are expected to be more reliable than those over grassland targets due to reduced spatial variability in spectral emissivity. However, comparisons over Tuttle Reservoir suggest that the at-

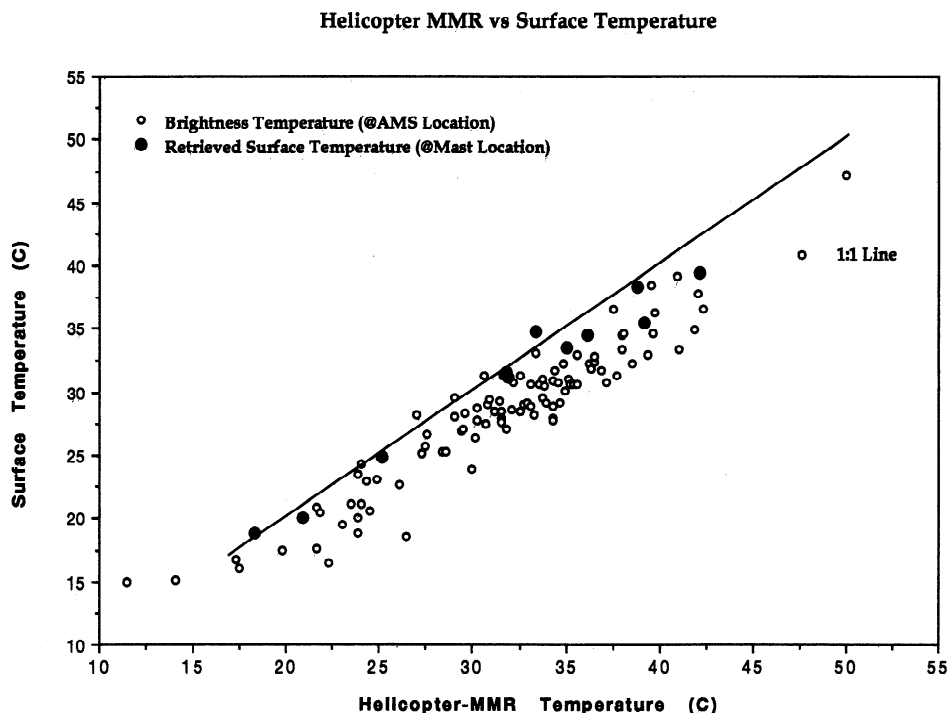


Figure 4. Helicopter MMR brightness temperatures ($N = 100$) and retrieved surface temperatures ($N = 11$) compared to coincident surface measurements for all available data during FIFE. See corresponding statistics in Tables 5a and 5b.

ospherically corrected TM brightness temperatures are at least 2.5°C warmer than surface measurements (the TM acquisition was one hour earlier than the surface measurements) and 3.5°C warmer than the coincident NS001 corrected brightness temperatures. Comparisons with coincident near-surface

temperatures from the mast-mounted instruments are consistent with these observations; the Landsat TM-retrieved surface temperatures overestimated comparable surface temperatures by +3.3° to +6.2°C (see Tables 4a, 4b, and 5b).

Sugita and Brutsaert [1993] also conducted a comparison of

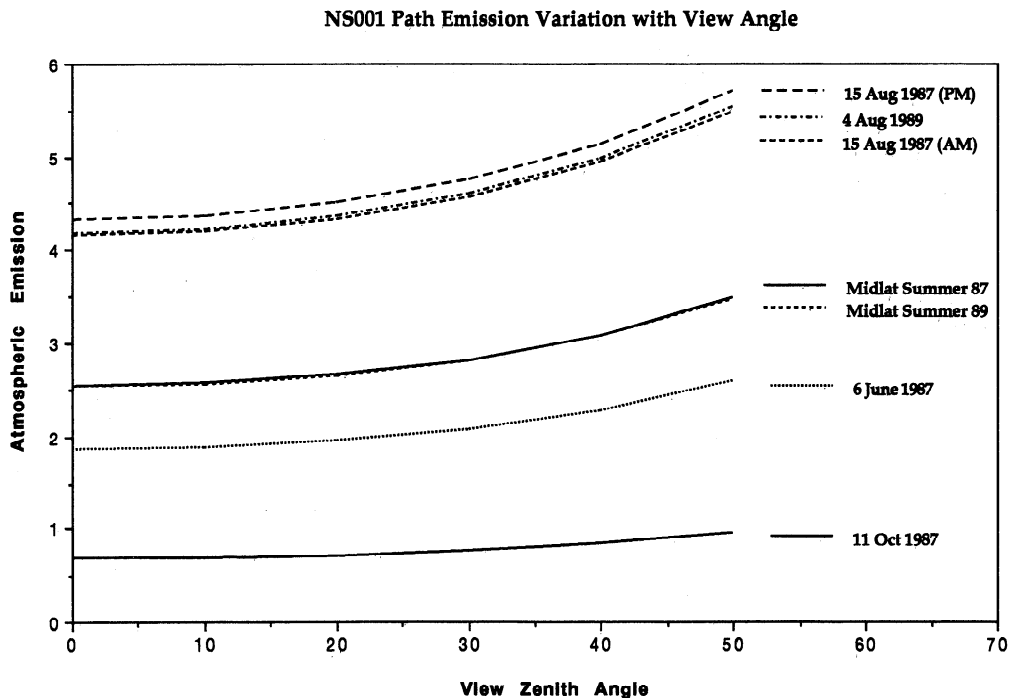


Figure 5a. Variation of atmospheric emission ($W m^{-2} sr^{-1} \mu m^{-1}$) with viewing angle (degrees), integrated over the NS001 relative sensor response, for several different specified atmospheres.

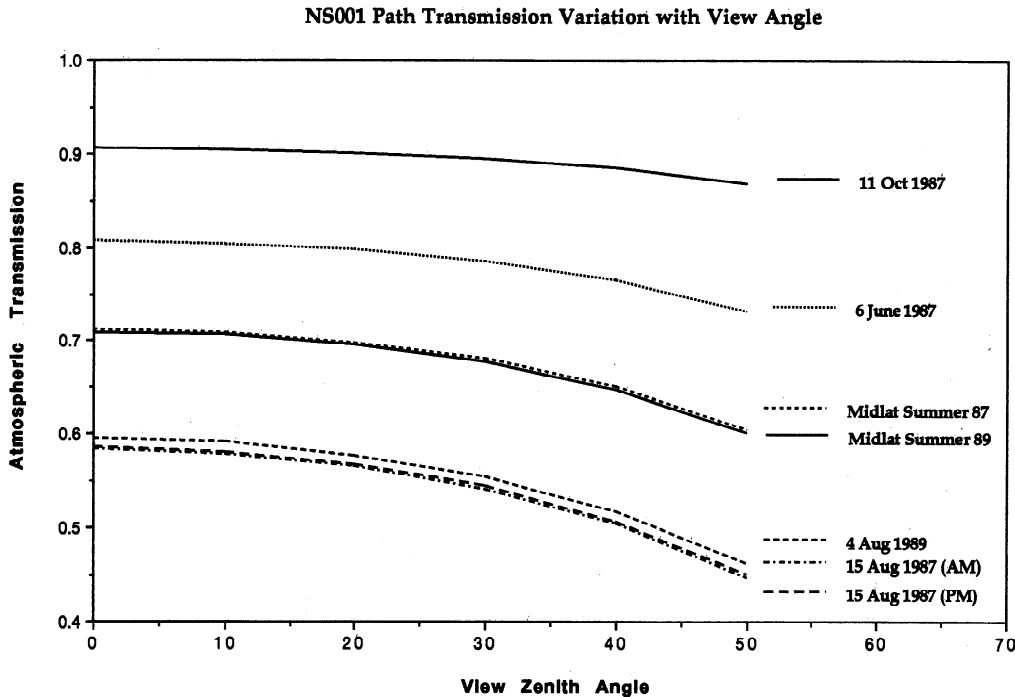


Figure 5b. Same as Figure 5a but for atmospheric path transmission.

surface radiometric temperatures retrieved from sensors of varying spatial resolution at the FIFE site. Root-mean-square “differences” between retrieved (atmospherically corrected) and measured surface temperatures were found to vary by sensor, from 3.1°C for the NOAA 9 AVHRR, 2.4°C for the NOAA 10 AVHRR, 2.2°C for NOAA 9 TOVS, 3.3°C for

NOAA 10 TOVS, 3.8°C for the GOES-VISSR, and 1.7°C for the Landsat 5 TM. All estimates were unbiased, with the exception of the TM, which systematically overestimated surface temperature. In the case of TM, atmospheric correction of the apparent at-sensor temperatures resulted in surface temperatures that deviated further from the observed surface temperature.

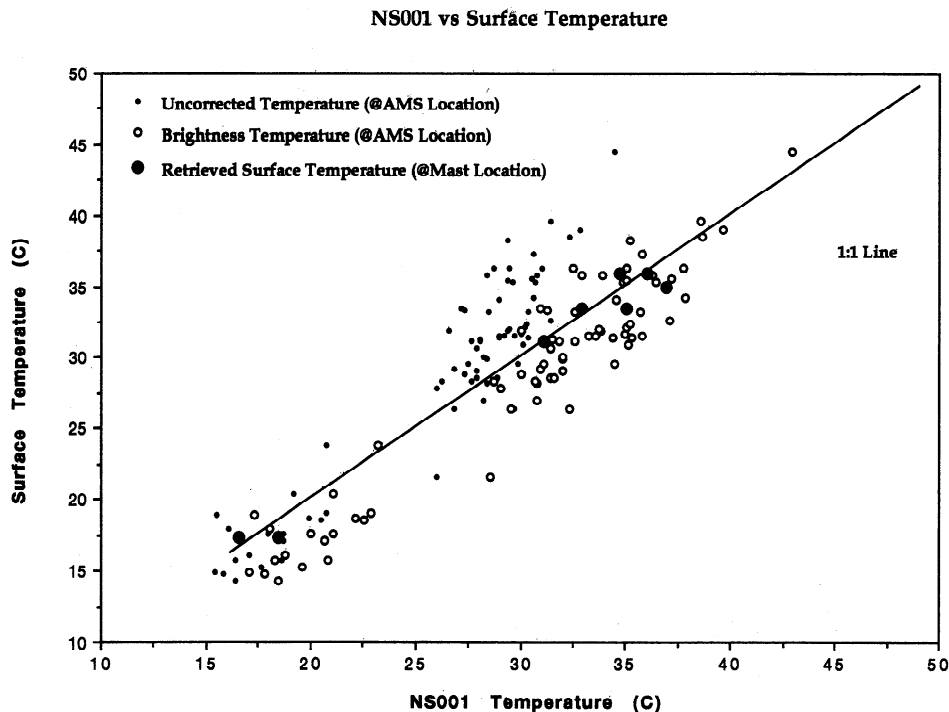


Figure 6. NS001-TMS brightness temperatures ($N = 65$) and retrieved surface temperatures ($N = 8$) compared to coincident surface measurements for all available data during FIFE. See corresponding statistics in Tables 5a and 5b.

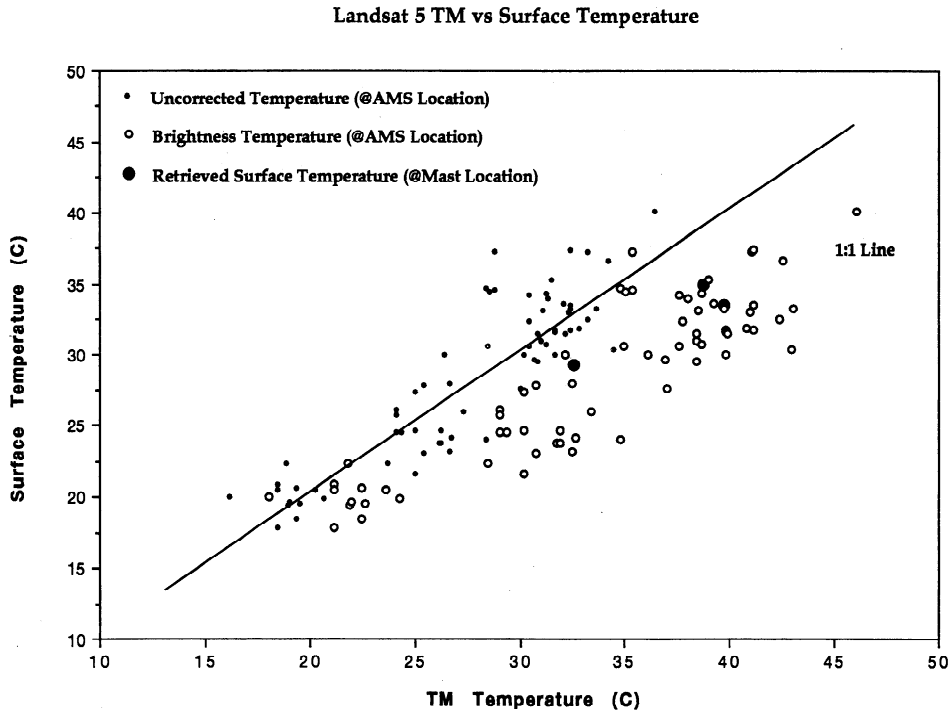


Figure 7. Landsat 5 TM brightness temperatures ($N = 67$) and retrieved surface temperatures ($N = 3$) compared to coincident surface measurements for all available data during FIFE. See corresponding statistics in Tables 5a and 5b.

In single-date analyses, *Schott and Volchok* [1985] also report a significant systematic error in surface temperatures derived from Landsat 4 and Landsat 5 TM. In the case of Landsat 4 there was an overestimation at observed low temperatures ($\sim 13^{\circ}\text{C}$) and an underestimation at higher temperatures ($\sim 21^{\circ}\text{C}$), with a crossover point around 17°C . The opposite trend was noted in Landsat 5 thermal data, over a greater range of temperatures ($\sim 10^{\circ}\text{--}40^{\circ}\text{C}$). In both Landsat 4 and Landsat 5 the difference between the measured and the retrieved temperatures were shown to be due to sensor internal calibration, in particular the gain. In Landsat 5 this resulted in a root-mean-square error of over 6°C , with the greatest errors at higher temperatures ($33^{\circ}\text{--}40^{\circ}\text{C}$). More frequent outgassing of the instrument was suggested as a means of alleviating possible moisture accumulation on the instrument's optical surfaces. Later analyses by *Schott* [1988] resulted in better agreement between retrieved and measured surface temperatures from Landsat 5, but residual concern was expressed over the sensor calibration due to an unrealistic requirement for atmospheric transmission values near 0.99.

For a series of dates between October 1985 and February 1988, *Wukelic et al.* [1989] compared retrieved surface temperatures from the Landsat 5 TM and surface measurements of water, vegetation and soil targets collected in Washington State. They found discrepancies between surface temperature measurements and retrieved TM radiometric temperatures of as much as 7.3°C . However, when adjustments for emissivity of generalized substrates were included, agreement between retrieved and measured surface temperatures were reduced to less than 1°C . We note that their emissivity correction results in retrieved temperatures lower than the brightness temperatures ($\epsilon = 1$), which is opposite of what would be expected from their correction formulae.

In our results, better agreement between the uncorrected TM apparent temperatures and surface measurements than with either the corrected brightness temperatures or the retrieved surface temperatures may be a result of either an over-correction for atmospheric attenuation or degradation of the TM thermal channel calibration. The magnitude of the atmospheric corrections is within expected ranges, averaging $+0.4^{\circ}\text{C}$ for the helicopter MMR, $+4.0^{\circ}\text{C}$ for the NS001, and $+6.1^{\circ}\text{C}$ for the TM. The close agreement between the retrieved NS001 temperatures and comparable near-surface temperature measurements of both water and grassland targets suggests that the atmospheric correction is handled well, including characterization of the atmosphere with local radiosonde profiles. This is reinforced by the fact that the majority of atmospheric attenuation is taking place in the atmospheric boundary layer (typically less than 2000 m above ground level), which is well below the nominal flying altitude of the C-130 in both 1987 and 1989 at the FIFE study area.

The abundance of coincident thermal data collected at the FIFE site and its multitemporal, multiscale characteristics, combined with independent confirmation of the results reported here, suggests that the portion of the atmospheric column between the surface and the sensor is well characterized by the radiosonde soundings, their use in the LOWTRAN-7 atmospheric radiance model, and the resulting retrieval of surface temperature from the apparent at-sensor radiances. We therefore calculated a revised calibration of the Landsat 5 TM thermal channel based on the comparison with FIFE AMS data. The resulting slope and offset terms are $0.05455 \text{ W m}^{-2} \text{ sr}^{-1} \mu\text{m}^{-1}$ and 0.93902 counts, respectively.

We note that spatial variability in the vegetation canopy may also introduce errors when comparisons are made at different spatial scales. The AMS instruments are measuring surface

temperature over just a 0.3 m² field of view in areas excluded from foot traffic or grazing. The mast-mounted instruments are sampling an area approximately 1.0 m² outside the AMS enclosure. The size of the surface area sampled by the helicopter MMR is slightly less than that sampled by the NS001 (see section 2.1), and the area sampled by the TM is significantly greater than that of either the MMR or the NS001 at the altitudes they were flown. However, the targets we examined are relatively homogeneous, particularly the reservoir, and there is no systematic change in corrected brightness temperatures consistent with changes in the spatial resolution of the various sensors.

5. Summary and Conclusions

Helicopter MMR and C-130 NS001 atmospherically corrected brightness temperatures are in general agreement with surface measurements at grassland targets over a wide range of site conditions and observation periods (Figures 2–6). The mean difference between NS001 and helicopter-MMR corrected brightness temperatures is 1.3°C, with the MMR systematically higher. The corrected helicopter MMR brightness temperatures overestimate those observed from AMS IRTs, with a mean difference of 3.2°C. An IRT mounted on the helicopter was in close agreement with the helicopter MMR uncorrected temperatures (0.8°C RMSE), suggesting the MMR was properly calibrated.

The corrected NS001 brightness temperatures overestimate the AMS IRT by 1.7°C but provide significantly more reliable estimates of surface temperature than the uncorrected values, particularly at higher temperatures (Figure 6). Furthermore, the range in corrected NS001 corrected brightness temperatures of the reservoir nicely bracket observed surface temperatures over a range of line transects (Table 3b).

Helicopter MMR and NS001-TMS data are in better agreement with coincident mast-mounted surface temperature measurements, all of which were corrected for surface emissivity and downwelling longwave radiation. Mean differences between the helicopter MMR and NS001 retrieved surface temperatures and the near-surface measurements were +0.9°C and +0.3°C, respectively (Figures 4 and 6). It is not clear why the retrieved aircraft surface temperatures are in excellent agreement with the near-surface temperatures observed from the mast-mounted instruments, yet the corrected brightness temperatures systematically overestimate the corresponding AMS IRT temperatures. There is no reason to suspect the validity of either the AMS, mast IRT, or MMR brightness temperatures (although it is likely the AMS IRTs observed a more vegetated (hence cooler) area).

In contrast to the results from the aircraft data we found that the Landsat 5 TM significantly overestimates not only the AMS IRT but also the mast-mounted IRT and MMR near-surface measurements and the reservoir temperatures. Use of revised TM calibration coefficients that we derived in place of the in-flight values results in accurate retrieval of surface temperatures from Landsat 5 TM data at the FIFE site. However, these calibration coefficients should not be generally applied to other regions. Instead, we recommend a rigorous reassessment of the Landsat 5 TM thermal channel calibration, and if appropriate, estimates of calibration degradation with time. This analysis is particularly important with the remote sensing community's increased reliance on continued useful operation of Landsat 5.

Acknowledgments. Numerous FIFE investigators are acknowledged for contributions to the data sets used in these analyses, particularly Blain Blad's group (University of Nebraska) for the mast measurements, Frank Palluconi's group (JPL) for the boat measurements, Charlie Walthall (UMD) for the helicopter acquisitions, and Wilf Brutsaert and M. Sugita (Cornell) for the radiosondes. Ralph Dubayah (UMD) is acknowledged for verifying the atmospheric corrections and three anonymous reviewers for providing several helpful suggestions.

References

- Bartolucci, L. A., M. Chang, P. E. Anuta, and M. R. Graves, Atmospheric effects of Landsat TM thermal IR data, *IEEE Transactions on Geoscience and Remote Sensing*, 26, 171–176, 1988.
- Berk, A., L. S. Bernstein, and D. C. Robertson, MODTRAN: A moderate resolution model for LOWTRAN 7, *Rep. AFGL-TR-89-0122*, Air Force Geophys. Lab., Bedford, Mass., 1989.
- Blad, B. L., E. A. Walter-Shea, C. J. Hays, and M. A. Mesarch, Calibration of field reference panel and radiometers used in FIFE 1989, *AgMet Progr. Rep. 90-3*, Dep. of Agric. Meteorol., Univ. of Nebraska, Lincoln, 1990.
- Brutsaert, W., Measurement and analysis of profiles through the atmospheric boundary layer through FIFE, *Rep. NAG5-1378*, Cornell Univ., Ithaca, N. Y., 1991.
- Choudhury, B. J., Estimating evaporation and carbon assimilation using infrared temperature data: Vistas in modeling, *Theory and Applications of Optical Remote Sensing*, edited by G. Asrar, pp. 628–690, John Wiley, New York, 1989.
- Cooper, D., and G. Asrar, Evaluating atmospheric correction models for retrieving surface temperature from the AVHRR over a tallgrass prairie, *Remote Sens. Environ.*, 27, 93–102, 1989.
- Friedl, M. A., and F. W. Davis, Sources of variation in radiometric surface temperature over a tallgrass prairie, *Remote Sens. Environ.*, 48, 1–17, 1994.
- Goetz, S. J., B. L. Markham, and J. E. Newcomer, Radiometric calibration and atmospheric correction of satellite and aircraft data for FIFE, *IGARSS '92, Remote Sens. Int. Geosci. Remote Sens. Symp.*, 1, 798–801, 1992.
- Goetz, S. J., F. G. Hall, B. L. Markham, and R. O. Dubayah, Intercomparison of retrieved surface temperature from multi-resolution sensors at the FIFE site, *Am. Soc. Photogrammetry Remote Sens.*, 2, 108–117, 1993.
- Hall, F. G., K. F. Huemmrich, S. J. Goetz, P. J. Sellers, and J. E. Nickeson, Satellite remote sensing of surface energy balance: Successes, failures and issues in FIFE, *J. Geophys. Res.*, 97, 19,061–19,089, 1992.
- Halthore, R. N., and B. L. Markham, Overview of atmospheric correction and radiometric calibration efforts during FIFE, *J. Geophys. Res.*, 97, 18,731–18,742, 1992.
- Hatfield, J. L., M. Vauclin, S. R. Vieira, and R. Bernard, Surface temperature variability patterns within irrigated fields, *Agric. Water Manage.*, 8, 429–437, 1984.
- Hays, C. J., M. A. Mesarch, and E. A. Walter-Shea, Surface temperatures, reflected and emitted radiation, and photosynthetically active radiation from the University of Nebraska, Lincoln, *FIFE Inf. Syst. Rep.*, Univ. of Neb., Lincoln, 1993.
- Jackson, R. D., D. A. Dusek, and C. E. Ezra, Calibration of the thermal channel on four Barnes model 1200 multi-modular radiometers, *WCR Rep. 12*, U.S. Dep. of Agric./Agric. Res. Serv., Phoenix, Ariz., 1983.
- Kimes, D. S., S. B. Idso, P. J. Pinter, R. J. Reginato, and R. D. Jackson, View angle effects in the radiometric measurement of plant canopy temperatures, *Remote Sens. Environ.*, 10, 273–284, 1980.
- Kneizys, F. X., E. P. Shettle, W. O. Gallery, J. H. Chetwynd, L. W. Abreu, J. E. A. Selby, S. A. Clough, and R. W. Fenn, Atmospheric transmittance/radiance: Computer code LOWTRAN 7, *AFGL-TR-88-0177*, Air Force Geophys. Lab., Hanscomb AFB, Mass., 1988.
- Kustas, W. P., R. D. Jackson, and G. Asrar, Estimating surface energy balance components from remotely sensed data, in *Theory and Applications of Optical Remote Sensing*, edited by G. Asrar, pp. 604–627, John Wiley, New York, 1989.
- Kustas, W. P., B. J. Choudhury, Y. Inoue, R. J. Pinter, M. S. Moran, R. D. Jackson, and R. J. Reginato, Ground and aircraft infrared observations over a partially-vegetated area, *Int. J. Remote Sens.*, 11(3), 409–427, 1990.
- Markham, B. L., and J. L. Barker, Landsat MSS and TM post-

- calibration dynamic ranges, exoatmospheric reflectances and at-satellite temperatures, *EOSAT Landsat Tech. Note, 1*, 3–8, 1986.
- Markham, B. L., F. M. Wood, and S. P. Ahmad, Radiometric calibration of the reflective bands of the NS001 thematic mapper simulator (TMS) and modular multiband radiometers (MMR), in *Recent Advances in Sensors, Radiometry and Data Processing for Remote Sensing*, pp. 96–108, SPIE—The Int. Soc. for Opt. Eng., Bellingham, Wash., 1988.
- Markham, B. L., R. N. Halthore, and S. J. Goetz, Surface reflectance retrieval from satellite and aircraft sensors: Results of sensor and algorithm comparisons during FIFE, *J. Geophys. Res.*, *97*, 18,785–18,795, 1992.
- Norman, J. M., J. Chen, and N. Goel, Thermal emissivity and infrared temperature dependence on plant canopy architecture and view angle, *IGARSS '90 Remote Sens. Int. Geosci. Remote Sens. Symp.*, 1747–1750, 1990.
- Palluconi, F., A. B. Kahle, G. Hoover, and J. E. Conel, *The Spectral Emissivity of Prairie and Pasture Grasses at Konza Prairie, Kansas*, Am. Meteorol. Soc., pp. 77–78, Boston, Mass., 1990.
- Palmer, J. M., Calibration of Thematic Mapper band 6 in the thermal infrared, in *Recent Publications Related to the Radiometric Calibration of Satellite and Airborne Multispectral Imaging Systems*, SPIE—The Int. Soc. for Opt. Eng., Bellingham, Wash., 1993.
- Price, J. C., Estimation of regional scale evaporation through analysis of satellite thermal infrared data, *IEEE Trans. Geosci. Remote Sens.*, *GE-20*, 286–292, 1982.
- Price, J. C., Estimating surface temperatures from satellite infrared data—A simple formulation for the atmospheric effect, *Remote Sens. Environ.*, *13*, 353–361, 1983.
- Richard, R. R., R. F. Merkel, and G. R. Meeks, NS001MS-Landsat-D thematic mapper band aircraft scanner, in *Proceeding of the 12th International Symposium on Remote Sensing of Environment*, Environ. Resour. Inst. of Mich., pp. 719–728, Ann Arbor, 1978.
- Schott, J. R., Thematic mapper, band 6, radiometric calibration and assessment, in *Recent Advances in Sensors, Radiometry, and Data Processing for Remote Sensing*, pp. 72–87, SPIE—The Int. Soc. for Opt. Eng., Bellingham, Wash., 1988.
- Schott, J. R., and W. J. Volchok, Thematic Mapper thermal infrared calibration, *Photogramm. Eng. Remote Sens.*, *51*(9), 1351–1357, 1985.
- Sellers, P. J., F. G. Hall, G. Asrar, D. E. Strebel, and R. E. Murphy, An overview of the First International Satellite Land Surface Climatology Project (ISLSCP) Field Experiment (FIFE), *J. Geophys. Res.*, *97*, 18,345–18,371, 1992.
- Sugita, M., and W. Brutsaert, Comparison of land surface temperatures derived from satellite observations with ground truth during FIFE, *Int. J. Remote Sens.*, *14*(9), 1659–1676, 1993.
- Vining, R. C., and B. L. Blad, Estimation of sensible heat flux from remotely sensed canopy temperatures, *J. Geophys. Res.*, *97*, 18,951–18,954, 1992.
- Walthall, C. L., *The FIFE helicopter mission*, FIFE Inf. Syst. Rep., Univ. of Md., College Park, 1988.
- Walthall, C. L., and E. M. Middleton, Assessing spatial and seasonal variations in grasslands with spectral reflectances from a helicopter platform, *J. Geophys. Res.*, *97*, 18,905–18,912, 1992.
- Wukelic, G. E., D. E. Gibbons, L. M. Martucci, and H. P. Foote, Radiometric calibration of Landsat Thematic Mapper thermal band, *Remote Sens. Environ.*, *28*, 339–347, 1989.

S. J. Goetz (corresponding author), F. G. Hall, R. N. Halthore, and B. L. Markham, NASA GSFC, Code 923, Biospheric Sciences Branch, Greenbelt, MD 20771.

(Received September 26, 1994; accepted October 4, 1994.)